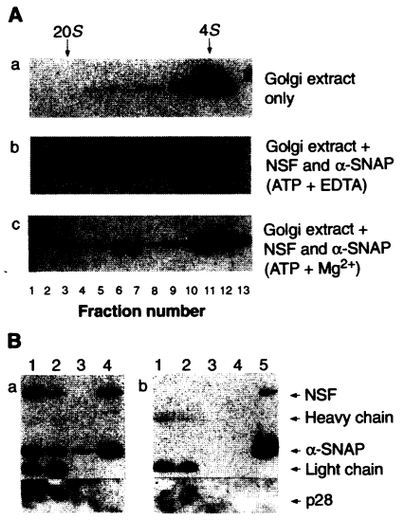

Fig. 4. p28 is part of the 20S Golgi SNARE complex. (**A**) Golgi extracts were incubated without (a) or with (b and c) NSF and α-SNAP in assembly (a and b) or disassembly buffer (c) and then separated on a 15 to 40% glycerol gradient. Gradient fractions were analyzed for the distribution of p28 by protein immunoblotting. BSA (4.6S) and α_2-macroglobulin (20S) were used as sedimentation standards. (**B**) The p28-containing 20S fractions were immunoprecipitated with mAb against p28 (a) or a control mAb (b) under the assembly condition. The immunoprecipitates were incubated in assembly (lanes 1 and 3) or disassembly buffer (lanes 2 and 4). The eluates (lanes 3 and 4) and the beads (lanes 1 and 2) were resolved by SDS-PAGE along with 100 ng of α-SNAP and NSF (lane 5) and then analyzed for the presence of NSF, α-SNAP, and p28 through the use of immunoblotting.

20S complex to be around 1 to 2:1:3 to 4 by comparing the result shown in Fig. 4B with standard curves of each protein in immunoblotting analysis, consistent with the observation that α-SNAP functions as a monomer whereas NSF acts as a homotrimer (*15*). p28 is thus a core component of the Golgi SNARE complex that participates in the docking or fusion stage of ER-Golgi transport (or both). Accordingly, we have renamed this protein GS28 (Golgi SNARE with a size of 28 kD). Because the primary sequence of GS28 is not significantly related to other known SNAREs, GS28 may represent a member of a distinct class of SNAREs that function in vesicle docking or fusion (or both). An unknown protein of 28 kD has been shown to be a component of the Golgi SNARE complex in yeast (*16*). Whether this yeast protein is related to GS28 awaits molecular characterization.

REFERENCES AND NOTES

1. J. E. Rothman, *Nature* **371**, 55 (1994); T. C. Sudhof, *ibid.* **375**, 645 (1995); N. K. Pryer, L. J. Wuestehube, R. Schekman, *Annu. Rev. Biochem.* **61**, 471 (1992); M. K. Bennett and R. H. Scheller, *ibid.* **63**, 63 (1994).
2. T. Söllner *et al.*, *Nature* **362**, 318 (1993).
3. D. W. Wilson *et al.*, *J. Cell Biol.* **117**, 531 (1992).
4. D. K. Banfield, M. J. Lewis, H. R. B. Pelham, *Nature* **375**, 806 (1995).
5. M. K. Bennett *et al.*, *Cell* **74**, 863 (1993); C. Dascher, J. Matteson, W. E. Balch, *J. Biol. Chem.* **269**, 29363 (1994).
6. V. N. Subramaniam *et al.*, *J. Cell Sci.* **108**, 2405 (1995).
7. Membrane proteins extracted from salt-washed rat liver Golgi membranes (*6*) were incubated with CNBr-Sepharose conjugated with mAb HFD9. p28 eluted from the beads was subjected to trypsin or endoproteinase GluC digestion. The resulting peptides were sequenced with a model 6600 ProSequencer (Milligen, Burlington, MA). One cDNA fragment of about 400 bp was obtained by PCR with a sense oligonucleotide [GA(T/C)AT(T/C/A)(T/C)TICA(A/G)GA(T/C)TA(T/C)ACICA] to peptide P4 (DILDYQTHE) and an antisense oligonucleotide [TG(A/G/T)ATIA(A/G)I(C/G)(A/T)(A/G)TTIACAGC IGG (A/G)AA] to peptide P9 (FPAVNSLIQR). This cDNA fragment was used to isolate a full-length rat cDNA clone (SKT7p28). Database searches were done with the BLAST program.
8. Transport assay was done exactly as described [C. J. M. Beckers, D. S. Keller, W. E. Balch, *Cell* **50**, 523 (1987); H. W. Davidson and W. E. Balch, *J. Biol. Chem.* **268**, 4216 (1993)].
9. The coding regions of p28cyto and cellubrevin minus the COOH-terminal transmembrane regions were amplified and cloned into pET23(d) (Novagen). This vector yields recombinant proteins with a COOH-terminal hexahistidine tag. Proteins were purified as recommended by the manufacturer.
10. H. T. McMahon *et al.*, *Nature* **364**, 346 (1993); T. Galli *et al.*, *J. Cell Biol.* **125**, 1015 (1994).
11. B. L. Tang *et al.*, *Eur. J. Cell Biol.* **65**, 298 (1994).
12. M. Aridor, S. I. Bannykh, T. Rowe, W. E. Balch, *J. Cell Biol.* **131**, 875 (1995); S. N. Pind *et al.*, *ibid.* **125**, 239 (1994); M. F. Rexach and R. W. Schekman, *ibid.* **114**, 219 (1991).
13. The 20S complex formation was done as described (*2, 3*). Salt-washed Golgi membranes were extracted with assembly buffer [20 mM Hepes-KOH (pH 7.4), 100 mM KCl, 2 mM dithiothreitol, 2 mM EDTA, 0.5 mM ATP, 0.5% (v/v) Triton X-100] or disassembly buffer (as above plus 8 mM $MgCl_2$). The extracts were then centrifuged at 100,000*g* in a TLA 100.2 rotor (Beckman) for 45 min and the supernatants retained. Recombinant His_6-NSF and His_6–α-SNAP were purified as described (*2, 3, 17*). Golgi extract (300 μg) was incubated with 60 μg of His_6-NSF and 15 μg of His_6–α-SNAP in a final volume of 500 μl. After a 30-min incubation at 4°C, the samples were loaded onto a 15 to 40% (w/v) glycerol gradient in the assembly (Fig. 4A) (a and b) or the disassembly buffer (c). Centrifugation was carried out for 18 hours in a SW41 rotor (Beckman). Fractions of about 0.8 ml were collected manually from the bottom at a flow rate of ~1 ml/min. Samples were resolved by SDS–polyacrylamide gel electrophoresis (SDS-PAGE), and the distribution of p28 was determined by immunoblotting.
14. Gradient fractions containing the 20S complex were diluted with assembly buffer containing 0.1% bovine serum albumin (BSA) and preincubated with protein G–Sepharose beads for 2 hours at 4°C followed by immunoprecipitation with either mAb HFD9 or mAb DAD5 (immunoglobulin G1 subtype control) bound to protein G–Sepharose. Beads were washed five times with assembly buffer containing 0.1% BSA, split into two equal portions, and incubated for 1 hour at room temperature with assembly buffer or disassembly buffer [assembly buffer containing 4 mM $MgCl_2$, 4 mM $CaCl_2$, and 25 μM guanosine triphosphate (GTP)]. The beads and supernatants were then processed for immunoblotting with antibodies to p28, α-SNAP, and NSF.
15. D. O. Clary, J. E. Rothman, *J. Biol. Chem.* **265**, 10109 (1990); S. W. Whiteheart *et al.*, *J. Cell Biol.* **126**, 945 (1994).
16. M. Sögaard *et al.*, *Cell* **78**, 936 (1994).
17. S. W. Whiteheart *et al.*, *Nature* **362**, 353 (1993).

18. We thank J. E. Rothman and W. E. Balch for reagents, C. Pallen, W. Chia, and members of W. Hong's laboratory for critical reading of the manuscript, and Y. H. Tan for his continuous support.

26 July 1995; accepted 28 March 1996

Vertical Flux of Biogenic Carbon in the Ocean: Is There Food Web Control?

Richard B. Rivkin,* Louis Legendre, Don Deibel, Jean-Éric Tremblay, Bert Klein, Kenneth Crocker, Suzanne Roy, Norman Silverberg, Connie Lovejoy, Fabrice Mesplé, Nancy Romero, M. Robin Anderson, Paul Matthews, Claude Savenkoff, Alain Vézina, Jean-Claude Therriault, Joel Wesson, Chantal Bérubé, R. Grant Ingram

Models of biogenic carbon (BC) flux assume that short herbivorous food chains lead to high export, whereas complex microbial or omnivorous food webs lead to recycling and low export, and that export of BC from the euphotic zone equals new production (NP). In the Gulf of St. Lawrence, particulate organic carbon fluxes were similar during the spring phytoplankton bloom, when herbivory dominated, and during nonbloom conditions, when microbial and omnivorous food webs dominated. In contrast, NP was 1.2 to 161 times greater during the bloom than after it. Thus, neither food web structure nor NP can predict the magnitude or patterns of BC export, particularly on time scales over which the ocean is in nonequilibrium conditions.

Between 30 and 50% of the CO_2 released from fossil fuel is removed from the atmosphere and exported from the ocean surface to depth as dissolved inorganic carbon and BC derived from primary production (PP) (*1–3*). The downward flux of BC from the ocean surface can be estimated directly from particulate organic carbon (POC) accumulation in sediment traps (*2, 4, 5*) or assessed indirectly (*5–7*) from

seasonal changes in dissolved nutrients or gases (such as NO_3, O_2, and CO_2) or in $^{234}Th/^{238}U$ disequilibrium, or from NO_3 uptake rates (ρNO_3) or the *f* ratio (*8*). The temporal and spatial patterns of PP, NP, and BC export have been characterized for various coastal and oceanic regions (*4*, *5*), and the relation between food web structure and direct or proxy indices of export has been modeled (*9*–*11*). These food web models predict that when large phytoplankton are abundant, herbivorous trophic pathways dominate and NP, *f* ratios, and BC export will be high; when small phytoplankton are abundant, microbial trophic pathways generally dominate and NP, *f* ratios, and BC export will be low (*10*–*13*). We tested these food web models in the Gulf of St. Lawrence (Fig. 1) by concurrently assessing the structure of the pelagic food web and determining BC fluxes by direct and indirect methods.

The food web structure differed significantly during and after the spring phytoplankton bloom (Table 1). In April, chlorophyll a concentrations (total and >5 μm), small heterotrophic nanoflagellate (HNAN) abundances, ρNO_3, *f* ratios, and rates of primary production and bacterial growth were high, and bacterial and ciliate abundances and the ratio of euphotic zone respiration to primary production (R:P) were low (*14*). The metabolism of the gulf was autotrophic (*15*). During the bloom, crustacean mesozooplankton were herbivorous and preferentially ingested large (>5 μm) particles (*16*, *17*). In late June, chlorophyll a concentrations (total and >5 μm), HNAN abundances, ρNO_3, *f* ratios, and rates of primary production and bacterial growth were generally low, and bacterial and ciliate abundances and R:P ratios were relatively high. The metabolism of the gulf was heterotrophic (*15*). During this postbloom period, the microbial food web was well developed, and crustacean mesozooplankton were presumably omnivorous, ingesting nonchlorophyllous prey of suitable size, such as heterotrophic dinoflagellates and ciliates (*18*).

Fluxes of chlorophyll a (*19*) and mesozooplankton fecal pellets (*20*) from the euphotic zone were 1.2 to 21 (mean = 8.4) times greater and 2.2 to 5.6 (mean =

R. B. Rivkin, D. Deibel, K. Crocker, P. Matthews, Ocean Sciences Centre, Memorial University of Newfoundland, St. John's, NF A1C 5S7, Canada.
L. Legendre, J.-É. Tremblay, B. Klein, C. Lovejoy, F. Mesplé, Département de biologie, Université Laval, Québec, QC G1K 7P4, Canada.
S. Roy, INRS-Océanologie, 310 Alée des Ursulines, Rimouski, QC G5L 3A1, Canada.
N. Silverberg, N. Romero, C. Savenkoff, A. Vézina, J.-C. Therriault, C. Bérubé, Institut Maurice-Lamontagne, Ministère des Pêches et des Océans, Casse Postale 1000, Mont-Joli, G5H 3Z4 QC, Canada.
M. R. Anderson, Marine Habitat Research, Science Branch, Fisheries and Oceans Canada, Newfoundland Region, Post Office Box 5667, St. John's, NF A1C 5X1, Canada.
J. Wesson and R. G. Ingram, Department of Atmospheric and Oceanic Sciences, McGill University, 805 Sherbrooke Street West, Montreal, QC H3A 2K6, Canada.
*To whom correspondence should be addressed.

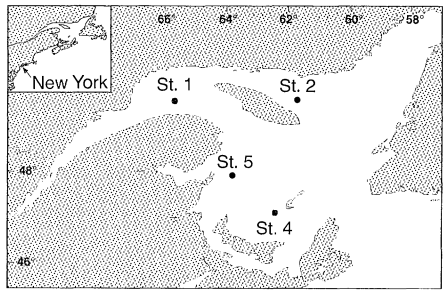

Fig. 1. Gulf of St. Lawrence study site and stations. St., station.

Table 1. Euphotic zone (1% isolume) values for selected physical and biological characteristics during bloom (10 to 22 April 1994) and nonbloom (13 to 24 June 1994) periods. Sampling locations and analytical protocols are in Fig. 1 and (*14*), respectively. Except as noted in (*14*), rates and standing stocks are euphotic zone averages (euphotic zone integrated values [per square meter] divided by euphotic zone depth [in meters]). New production was computed as in (*8*) from *f* ratios and ρNO_3. The Wilcoxon's signed rank test was used to assess differences between stations during different seasons (asterisk indicates $P \leq 0.05$; NS, not significant; ND, not determined).

Station	Bloom				Nonbloom				Significance test
	1	2	4	5	1	2	4	5	
Euphotic zone stability—($\sigma t_{surface} - \sigma t_{1\%\ isolume}$)†	0.4	0.4	0.5	0.1	3.5	2.1	1.7	2.9	*
Euphotic zone depth (m)	26	33	31	17	30	54	33	13	NS
Total chlorophyll a (mg m^{-3})	2.1	2.9	0.6	7.6	0.4	0.1	0.4	1.3	*
Chlorophyll a >5 μm (%)	57	81	53	95	18	13	0.2	62	*
POC (mg m^{-3})	215	196	150	530	287	140	232	386	NS
PON (mg m^{-3})	37	38	25	101	51	30	51	75	NS
PP (mg of C m^{-3} day^{-1})	210	72	41	222	7	3	11	16	*
PP > 5 μm (%)	ND	99	49	100	30	9	12	43	*
NO_3 uptake (ρNO_3; μmol m^{-3} day^{-1})	2075	882	174	2796	46	8.2	147	87	*
f ratio	0.85	0.73	0.55	0.78	0.16	0.07	0.45	0.09	*
New production (mg of C m^{-3} day^{-1}) [PP × *f* ratio; (ρNO_3 × 79.2)]	178; 164	53; 70	23; 14	173; 219	1.1; 3.7	0.2; 0.6	4.9; 11	1.4; 6.8	*
New production: POC flux ratio [PP × *f* ratio:POC; (ρNO_3 × 79.2):POC]	32; 29	14; 18	4; 6	36; 46	0.2; 0.7	0.1; 0.4	1.3; 3.1	0.1; 0.5	
Bacterial abundance (10^{11} cells m^{-3})	3.8	1.9	3.5	5.2	12.9	3.8	9.1	17.3	*
Bacterial growth rate (day^{-1})	0.55	0.42	0.42	0.48	0.12	0.21	0.33	0.19	*
Bacteria:phytoplankton biomass ratio (C:C)	0.11	0.16	0.23	0.04	2.04	1.09	0.99	0.58	*
Respiration:PP (C:C)	0.05	0.14	0.17	0.10	1.3	1.6	0.7	1.1	*
Ciliates (cells ml^{-1})	0.1	0.6	0.4	1.8	5.3	2.3	6.8	4.2	*
Heterotrophic dinoflagellates (cells ml^{-1})	4.5	5.9	1.5	11.1	30.0	1.7	2.8	3.7	NS
HNAN <5 μm (cells ml^{-1})	13.0	6.2	1.6	12.0	<0.1	1.2	<0.1	<0.1	*
HNAN >5 μm (cells ml^{-1})	1.0	<0.1	0.2	0.6	13.2	0.2	2.9	9.9	*
Bacterial grazing mortality (day^{-1})	0.61	ND	0.52	0.48	0.06	ND	0.12	0.08	*
Mesozooplankton biomass 500 to 2000 μm (g m^{-2})	6.9	0.9	2.0	ND	2.0	2.2	13.1	2.6	NS

†σt is the density of seawater defined as (specific gravity at temperature in degrees Celsius − 1) × 1000.

3.5) times smaller, respectively, during than after the phytoplankton bloom (Fig. 2). In contrast, fluxes of POC and particulate organic nitrogen (PON) were similar in the two seasons. Euphotic zone export of BC computed from f ratios and ρNO_3 (8) was 1.2 to 161 (mean = 52) times greater in April than in June, and the resultant NP:POC flux ratio was 4 to 46 (mean = 23) during the bloom and 0.1 to 3.1 (mean = 0.8) after the bloom (Table 1). Although we assume that BC export can be estimated from POC collected in surface-tethered sediment traps, because of collection and hydrodynamic bias, particle fluxes computed from traps data may be 1.1 to 3 times greater than those predicted by ^{234}Th profiles (3, 21).

In Fig. 3, we propose a conceptual model of food web control of BC export. During the bloom, large phytoplankton are abundant (Table 1) and mesozooplankton are primarily herbivorous (16). There is a large downward flux of aggregated phytoplankton and a moderate flux of mesozooplankton fecal pellets (Fig. 2). At low ambient temperatures, the growth of ciliates is depressed and their abundances are low (22). Top-down grazing control on small (<5 μm) HNAN by ciliates is weak, hence HNAN are abundant. In general, only small HNAN ingest bacteria, whereas larger HNAN are predominantly herbivorous (23). Although bacterial growth rates are high, bacterial abundances are low because mortality caused by the grazing of numerous small HNAN equals or exceeds bacterial growth rates. During substrate addition studies, bacterial growth was not stimulated by micromolar additions of glucose or glutamate (24), which suggests that ambient concentrations of substrate did not limit bacterial growth. The observed high growth rates were sustained by dissolved organic carbon (DOC) released by phytoplankton, by sloppy feeding by mesozooplankton, and by the production of DOC and dissolved organic nitrogen (DON) as byproducts of micro- and mesozooplankton metabolism (25). After the bloom, large phytoplankton are scarce (Table 1) and mesozooplankton are primarily omnivorous and ingest nonchlorophyllous prey such as large flagellates and ciliates (18). The downward flux is dominated by fecal pellets (Fig. 2). At the relatively high seawater temperatures (22), ciliates' growth rates may exceed their grazing mortality. Because of the top-down grazing control by the abundant ciliates, small HNAN are scarce (Table 1). Hence, despite slower growth rates, bacteria accumulate because grazing mortality is <50% of their growth rate. Substrate addition studies (24), in which bacteria were stimulated by glutamate but not glucose, suggest that DON or NH_4 limited bacterial growth. Mesozooplankton abundances were not significantly different in mid-April and late June (Table 1), and it is likely that the release

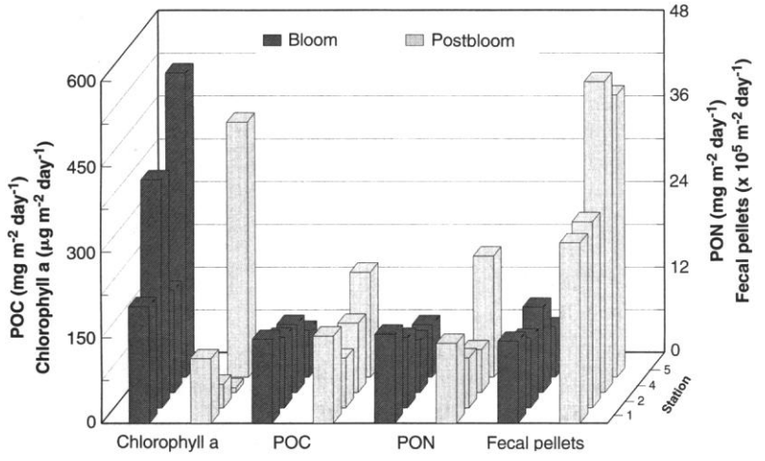

Fig. 2. Downward fluxes of chlorophyll a, POC, nitrogen (PON), and fecal pellets (19).

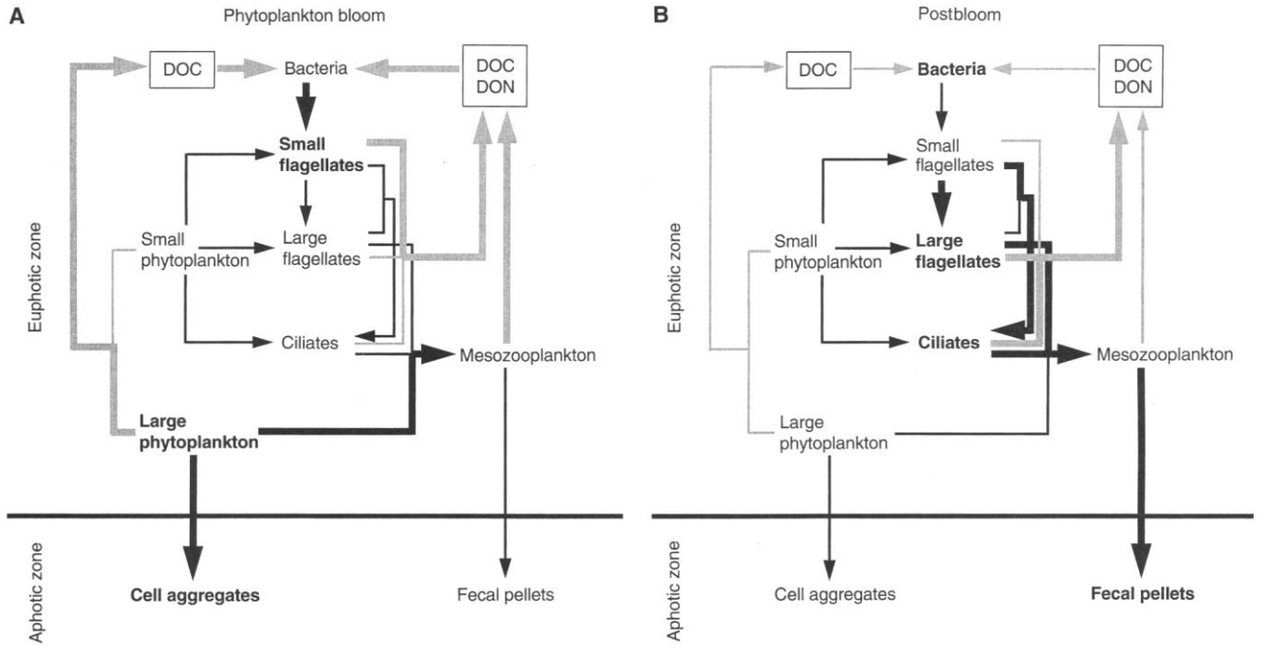

Fig. 3. Conceptual model of the interactions between food web structure and BC export in the Gulf of St. Lawrence during and after the spring phytoplankton bloom. The interactions, based on Table 1 and Fig. 2, are discussed in the text. Solid and shaded arrows denote fluxes of particulate and dissolved organic material, respectively. Wide arrows and bold type represent large fluxes and high standing stocks, respectively.

rate of DON and NH_4 by crustacean mesozooplankton was insufficient to sustain high bacterial growth rates. This conclusion is consistent with an approximately twofold greater nitrogen assimilation efficiency of copepods when ingesting nonchlorophyllous prey (90 to 99%), such as ciliates, than when feeding on phytoplankton (35 to 62%) (*26*).

Our results, which contrast with food web model predictions of generally higher BC export by herbivorous than microbial food webs (*9–11*), suggest that: (i) The seasonal progression from an autotrophic to a heterotrophic pelagic food web was accompanied by the replacement of the size class occupied by large phytoplankton in April with large dinoflagellates and ciliates in June. This enabled mesozooplankton to shift from herbivory, when large phytoplankton were abundant, to omnivory, when the microbial food web dominated (*18*). (ii) POC and PON export were similar during the bloom, when phytoplankton and herbivorous grazing pathways dominated, and during nonbloom conditions, when planktonic heterotrophs and microbial pathways dominated (*13*). There was a concomitant change in the flux composition and relative dominance from chlorophyllous material in April to fecal pellets in June. (iii) In April, POC export was <10% of primary production, and in June it was 10 to 35%. Thus, in some circumstances, heterotrophic systems can export more biogenic carbon, relative to primary production, than can autotrophic systems. (iv) There were significant discrepancies between BC export computed as NP (*8*) and that determined directly as POC in sediment traps. Part of this discrepancy may be due to fluxes of DOC during the spring bloom (*3*, *27*). Thus, estimating export of BC from ρNO_3 or *f* ratios assessed over short (for instance, seasonal) time scales (*28*), or for systems which are not in a steady state, may be subject to large uncertainties (*8*, *9*, *29*). We conclude that BC export can be independent of the trophic mode (*13*) of the plankton, and neither food web structure nor observational scale estimates of NP (*8*) can be used to predict the magnitude or pattern of BC export from the ocean surface.

REFERENCES AND NOTES

1. P. P. Tans, I. Y. Fung, T. Takahashi, *Science* **247**, 1431 (1990).
2. S. E. Lohrenz *et al.*, *Deep Sea Res.* **39**, 1373 (1992).
3. A. F. Michaels, N. R. Bates, K. O. Buesseler, C. A. Carlson, A. H. Knap, *Nature* **371**, 537 (1994).
4. M. L. Pace, G. A. Knauer, D. M. Karl, J. H. Martin, *ibid.* **325**, 803 (1987); A. F. Michaels *et al.*, *Deep Sea Res.* **41**, 1013 (1994).
5. R. W. Eppley, in *Productivity of the Ocean, Present and Past*, W. H. Berger, V. S. Smetacek, G. Wefer, Eds. (Wiley, New York, 1989), pp. 85–97.
6. R. C. Dugdale, F. P. Wilkerson, R. T. Barber, F. P. Chavez, *J. Geophys. Res.* **97**, 681 (1992).
7. R. W. Eppley and B. J. Peterson, *Nature* **282**, 677 (1979).
8. *f* equals nitrate uptake as a fraction of total inorganic nitrogen uptake [$\rho NO_3/(\rho NO_3 + \rho NH_4 + \rho Urea)$] where ρ = uptake rate [Y. Collos, *Int. J. Radiat. Appl. Inst.* **38**, (1987)]: NP = PP × *f* ratio. Alternatively, NP can be computed as $\rho NO_3 \times$ C:N × 12, where the C:N of phytoplankton = 6.6 [S. C. Redfield, B. H. Ketchum, F. A. Richards, in *The Sea*, M. N. Hill, Ed. (Wiley, New York, 1963), pp. 26–77]. NP computed from ^{15}N uptake may reflect transient rather than steady-state characteristics. On the Scotian Shelf (eastern Canada), NP computed from the *f* ratio becomes equivalent to BC export when integrated on time scales greater than 6 months (S. Dauchez, L. Legendre, L. Fortier, M. Levasseur, *Mar. Ecol. Prog. Ser.*, in press.)
9. L. Legendre and M. Gosselin, *Limnol. Oceanogr.* **34**, 1374 (1989).
10. A. Hagstrom, F. Azam, A. Andersson, J. Wilkner, F. Rassoulzadegan, *Mar. Ecol. Prog. Ser.* **49**, 171 (1988); A. H. Taylor and I. Joint, *ibid.* **59**, 1 (1990); L. Legendre and J. Le Fèvre, *Aquat. Microb. Ecol.* **9**, 69 (1995).
11. An exception is when mucous web feeders are abundant [A. F. Michaels and M. W. Silver, *Deep Sea Res.* **35**, 473 (1988)].
12. Photosynthetic nano- and picoplankton and bacteria are ingested by heterotrophic flagellates, which in turn are ingested by ciliates [F. Azam *et al.*, *Mar. Ecol. Prog. Ser.* **10**, 257 (1983)].
13. L. Legendre and F. Rassoulzadegan [*Ophelia* **41**, 153 (1995)] regard the herbivorous and microbial trophic pathways as extremes of the trophic continuum. Thus, herbivory, omnivory, and bacterivory can cooccur, and the ratios of export (NP) or regenerated to total production would depend on the relative dominance of the different trophic modes.
14. Euphotic zone stability and depth were determined with a Seabird SBE 25 Sealogger CTD and a LiCor quantum photometer, respectively. Water samples were normally collected before sunrise from the surface and from five photic depths (50, 25, 15, 10, and 1% of incident irradiance). Total and size-fractionated chlorophyll a, POC, PON, daily primary production (incorporation of $NaH^{14}CO_3$), ρNO_3, and *f* ratios (sequential 6-hour incubations with ^{15}N) were determined according to J.-E. Tremblay, B. Klein, L. Legendre, R. B. Rivkin, and J.-C. Therriault (*Limnol. Oceanogr.*, in press). Bacterial abundances were determined from acridine orange direct counts [J. E. Hobbie, R. J. Daley, S. Jasper, *Appl. Environ. Microbiol.* **33**, 1225 (1977)]. Phytoplankton and bacterial carbon were estimated with the assumption that the ratio of carbon to chlorophyll a was 50 and that there were 20 fg of carbon per cell, respectively. Bacterial growth rates were calculated from incorporation of ^3H-thymidine, with the use of empirical conversion factors to transform thymidine incorporation into cell production [D. Kirchman, H. Ducklow, R. Mitchell, *ibid.* **44**, 1296 (1982)]. Respiration of the <200 μm size fraction was estimated from electron transport system activity with the use of the empirical relation (r^2 = 0.75, $P < 0.001$) from J. Aristegui and M. F. Montero [*J. Plank. Res.* **17**, 1563 (1995)] and a respiratory quotient equal to 1. Ciliate and flagellate abundance were determined by epifluorescence microscopy from glutaraldehyde-preserved samples. Bacterial grazing mortality in the <200 μm size fraction was determined from dilution assays [M. R. Landry and R. P. Hasset, *Mar. Biol.* **67**, 283 (1982)]. Mesozooplankton collected during vertical net (0.5 m diameter WP-2 net with 200-μm aperture) hauls (0 to 150 m at stations 1 and 2 and 0 to 60 m at stations 4 and 5) were screened and then dried at 60°C, and the dry weight was converted to carbon biomass with the use of size-dependent empirical relations.
15. S. V. Smith and J. T. Hollibaugh, *Rev. Geophys.* **31**, 75 (1993).
16. During these cruises, the selection efficiency {[($CR_{algae\ <3\ \mu m}/CR_{algae\ 20\ to\ 65\ \mu m}$) × 100]; CR, clearance rate} of the dominant copepods was 1 to 44% (median = 4.8%, n = 9) in both seasons. This implies that large phytoplankton were preferentially ingested whenever they were present [K. Crocker, unpublished data].
17. M. M. Mullin, *Limnol. Oceanogr.* **8**, 239 (1963); B. W. Frost, *ibid.* **17**, 805 (1972).
18. D. J. Gifford and M. J. Dagg, *Mar. Microb. Food Webs* **5**, 161 (1991); M. D. Ohman and J. A. Runge, *Limnol. Oceanogr.* **39**, 21 (1994).
19. Sediment trap arrays of four 78-cm^2 tubes (aspect ratio = 10:1) were deployed below the euphotic zone, at about 50 m, for 24 hours. Fresh trap material was microscopically examined, combined and concentrated by settling and centrifugation, and split for subsequent determination of POC, PON (CHN analysis), and chlorophyll a (by high-performance liquid chromatography) [S. W. Wright *et al.*, *Mar. Ecol. Prog. Ser.* **77**, 183 (1991)], and for microscopic enumeration of fecal pellets.
20. The total volume of mesozooplankton fecal pellets collected in the traps was 2.9 to 6.5 (mean = 3.9) times smaller during than after the bloom.
21. K. O. Buesseler, *Nature* **353**, 420 (1991); B. Paul and J. W. Murray, *Eos* **76**, 6 (1996).
22. Temperatures in the surface layer were −1.6° to −0.5°C during the bloom and 7.5° to 11°C after the bloom. Ingestion and growth rates of ciliates are highly sensitive to temperature (Q_{10} = 3.5 to 5.4) [F. Rassoulzadegan, *Ann. Inst. Oceanogr. Paris* **58**, 177 (1982); C. M. Aelion and S. W. Chisholm, *J. Plank. Res.* **7**, 821 (1985)]. In contrast, growth rates of HNAN from seasonally cold oceans are >0.5 per day at −1.8°C [J. W. Choi and F. Peters, *Appl. Environ. Microbiol.* **58**, 593 (1992)].
23. Sherr and Sherr reported that >88% of bacteriverous HNAN are <5 μm [B. F. Sherr and E. B. Sherr, *Mar. Microb. Food Webs* **5**, 227 (1991)], whereas larger HNAN preferentially ingest pico- and nanophytoplankton [*Microb. Ecol.* **28**, 223 (1994)].
24. With the use of a factorial matrix, seawater dilution cultures (<1-μm filtrate diluted 1:5 with 0.2-μm filtrated seawater) were amended with glucose or glutamic acid (2.5 μmol $liter^{-1}$) (plus an unamended control), and the time course change in bacterial abundance was measured for 72 to 96 hours [R. B. Rivkin, M. R. Anderson, D. E. Gustafson, *Antarct. J. U.S.* **26**, 145 (1991); R. B. Rivkin, unpublished data].
25. P. A. Jumars, D. L. Perry, J. A. Baross, M. J. Perry, B. W. Frost, *Deep Sea Res.* **36**, 483 (1989).
26. E. D. S. Corner, C. B. Cowey, S. M. Marshall, *J. Mar. Biol. Assoc. U. K.* **47**, 259 (1967); E. D. S. Corner, R. N. Head, C. C. Kilvington, L. Pennycuick, *ibid.* **56**, 345 (1976).
27. C. A. Carlson, H. W. Ducklow, A. F. Michaels, *Nature* **371**, 405 (1994).
28. This is the approach generally used in models employing remotely sensed data [T. Platt and S. Sathyendranath, *Science* **241**, 1613 (1988); R. C. Dugdale, A. Morel, A. Bricaud, F. R. Wilkerson, *J. Geophys. Res.* **94**, 18119 (1989); S. Sathyendranath *et al.*, *Nature* **353**, 129 (1991)].
29. Export and NP are equivalent on spatial and temporal scales, which are larger than those generally used during most field and modeling studies [T. Platt *et al.*, *Mar. Ecol. Prog. Ser.* **52**, 77 (1989)].

30. This research was done as a contribution to the programs of the Ocean Sciences Centre, GIROQ (Groupe interuniversitaire de recherches océanographiques du Québec), and the Maurice Lamontagne Institute, Department of Fisheries and Oceans (DFO), Canada. The research was part of the Canadian Joint Global Ocean Flux Study program, whose principal support comes from the Natural Sciences and Engineering Research Council of Canada and the DFO. We thank A. Bedi, H. Chen, M.-L. Dubé, L. Dyer, A. Gagné, C. LeDrew, S. Mazumber, S. Noonan, P. Peltolla, M. Riehl and N. Simard for technical assistance and acknowledge the contributions of the captains and crews of the research vessel *CSS Hudson* (DFO) and the Canadian Coast Guard icebreaker *Sir Wilfrid Laurier* for assistance with sample collection and sediment trap deployment and retrieval.

12 October 1995; accepted 26 February 1996